Band Gap Tunable, Donor−Acceptor−Donor Charge-Transfer Heteroquinoid-Based Chromophores: Near Infrared Photoluminescence and Electroluminescence

Gang Qian,[†,‡] Bo Dai,[†,‡] Min Luo,[†,‡] Dengbin Yu,[†] Jie Zhan,[†,‡] Zhiqiang Zhang,[†] Dongge Ma,[†] and Zhi Yuan Wang*[,†,§]

State Key Laboratory of Polymer Physics and Chemistry, Changchun Institute of Applied Chemistry, Chinese Academy of Sciences, and Graduate School of Chinese Academy of Sciences, Changchun 130022, China, and Department of Chemistry, Carleton University, 1125 Colonel By Drive, Ottawa, Ontario, Canada K1S 5B6

Received June 7, 2008

A series of D-π-A-π-D type of near-infrared (NIR) fluorescent compounds based on benzobis(thiadiazole) and its selenium analogues were synthesized and fully characterized by ^{1}H and ^{13}C NMR, high-resolution mass spectrometry, and elemental analysis. The absorption, fluorescence, and electrochemical properties were also studied. Photoluminescence of these chromophores ranges from 900 to 1600 nm and their band gaps are between 1.19 and 0.56 eV. Replacing the sulfur by selenium can lead to a red shift for emission and reduce the band gaps further. Interestingly, compound **1** exhibits aggregation-induced emission enhancement effect in the solid state. All-organic light-emitting diodes based on **M1** and **M2** were made and exclusive NIR emissions above 1 μm with external quantum efficiency of 0.05% and maximum radiance of 60 mW Sr^{-1} m^{-2} were observed. The longest electroluminescence wavelength reaches 1115 nm.

Introduction

Near-infrared (NIR) fluorescent organic compounds are an emerging class of materials with potential applications as NIR fluorescent tags for bioimaging and sensing or emitters in NIR light-emitting diodes (LEDs) for information-secured display and background lighting. To date, much effort has been made to achieve the emission above 700 nm mainly with lanthanide complexes,[1] transition metal complexes,[2] ionic dyes,[3] and low band gap polymers.[4] However, because of the parity-forbidden radiative 4f−4f transitions of the rare earth ions, the external quantum efficiency (EQE) of these LEDs were rather low and the driving voltages were quite high. Replacing the fluorescent materials with phosphorescent complexes could increase the EQE remarkably. Borek et al.[2a] reported a Pt-based porphyrin complex with high EQE (6.3%), but the LED emits only at 765 nm or still visibly deep red color. Cheng et al.,[2c] Guo et al.,[2e] and Rosenow et al.[2d] reported LEDs based on heavy-metal phthalocyanines which emit at about 1 μm; however, the devices have low EQE at the NIR wavelength and emit strong visible light. Suzuki et al.[3d] reported the electroluminescence (EL) at around 1100 nm based on the NIR dyes doped in polymer and the optimized efficiency of 0.036%. A LED based on low band gap polymers described by Chen et al.[4e] emitted the light peaked at 970 nm with the EQE of 0.03−0.05%. With use of InAs/ZnSe nanoparticles-doped polymers, a LED can emit the light at 1300 nm with EQE of 0.5%.[5] Therefore, it still remains challenging to realize high-efficiency NIR photoluminescence (PL) for organic compounds and in particular EL, without any visible light, from all-organic LEDs at wavelengths beyond 1000 nm.

* To whom correspondence should be addressed. E-mail: wayne_wang@carleton.ca.
† Changchun Institute of Applied Chemistry, Chinese Academy of Sciences.
‡ Graduate School of Chinese Academy of Sciences.
§ Carleton University.

(1) (a) Kido, J.; Okamoto, Y. *Chem. Rev.* **2002**, *102*, 2357. (b) Zang, F. X.; Hong, Z. R.; Li, W. L.; Li, M. T.; Sun, X. Y. *Appl. Phys. Lett.* **2004**, *84*, 2679. (c) Slooff, L. H.; Polman, A.; Cacilli, F.; Friend, R. H.; Hebbink, G. A.; van Veggel, F. C. J. M.; Reinhoudt, D. N. *Appl. Phys. Lett.* **2001**, *78*, 2122. (d) Curry, R. J.; Gillin, W. P. *Appl. Phys. Lett.* **1999**, *75*, 1380. (e) Kang, T.-S.; Harrison, B. S.; Foley, T. J.; Knefely, A. S.; Boncella, J. M.; Reynolds, J. R.; Schanze, K. S. *Adv. Mater.* **2003**, *15*, 1093.

(2) (a) Borek, C.; Hanson, K.; Djurovich, P. I.; Thompson, M. E.; Aznavour, K.; Bau, R.; Sun, Y.; Forrest, S. R.; Brooks, J.; Michalski, L.; Brown, J. J. *Angew. Chem., Int. Ed.* **2007**, *46*, 1109. (b) Sun, Y.; Borek, C.; Hanson, K.; Djurovich, P. I.; Thompson, M. E.; Brooks, J.; Brown, J. J.; Forrest, S. R. *Appl. Phys, Lett.* **2007**, *90*, 213503. (c) Cheng, C. H.; Fan, Z. Q.; Yu, S. K.; Jiang, W. H.; Wang, X.; Du, G. T.; Chang, Y. C.; Ma, C. Y. *Appl. Phys. Lett.* **2006**, *88*, 213505. (d) Rosenow, T. C.; Walzer, K.; Leo, K. *J. Appl. Phys.* **2008**, *103*, 043105. (e) Guo, Z. G.; Cheng, C. H.; Fan, Z. Q.; He, W.; Yu, S. K.; Chang, Y. C.; Du, X. G.; Wang, X.; Du, G. T. *Chin. Phys. Lett.* **2008**, *25*, 715.

(3) (a) Casalboni, M.; De Matteis, F.; Prosposito, P.; Pizzoferrato, R. *Appl. Phys. Lett.* **1999**, *75*, 2172. (b) Suzuki, H. *Appl. Phys. Lett.* **2000**, *76*, 1543. (c) Suzuki, H. *Appl. Phys. Lett.* **2002**, *80*, 3256. (d) Suzuki, H.; Ogura, K.; Matsumoto, N.; Prosposito, P.; Schutzmann, S. *Mol. Cryst. Liq. Cryst.* **2006**, *444*, 51.

(4) (a) Yang, R.; Tian, R.; Yan, J.; Zhang, Y.; Yang, J.; Hou, Q.; Yang, W.; Zhang, C.; Cao, Y. *Macromolecules* **2005**, *38*, 244. (b) Li, X.; Zeng, W.; Zhang, Y.; Hou, Q.; Yang, W.; Cao, Y. *Eur. Polym. J.* **2005**, *41*, 2923. (c) Thompson, B. C.; Madrigal, L. G.; Pinto, M. R.; Kang, T.-S.; Schanze, K. S.; Reynolds, J. R. *J. Polym. Sci., Part A: Polym. Chem.* **2005**, *43*, 1417. (d) Baigent, D. R.; Hamer, P. J.; Friend, R. H.; Moratti, S. C.; Holmes, A. B. *Synth. Met.* **1995**, *71*, 2175. (e) Chen, M.; Perzon, E.; Andersson, M. R.; Marcinkevicius, S.; Jönsson, S. K. M.; Fahlman, M.; Berggren, M. *Appl. Phys. Lett.* **2004**, *84*, 3570.

(5) Tessler, N.; Medvedev, V.; Kazes, M.; Kan, S.; Banin, U. *Science* **2002**, *295*, 1506.

10.1021/cm801911n CCC: $40.75
Published on Web 09/18/2008

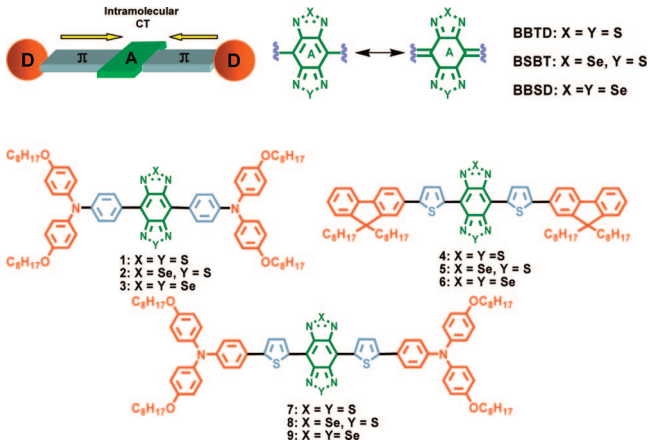

Figure 1. Design concept for D−A−D chromophores with three acceptors (top) and chemical structures of NIR chromophores **1**−**9** (bottom).

Among many low band gap organic compounds, the donor−acceptor (D−A) type of chromophores are particularly of interest to us as potential NIR chromophores because their band gap levels and other properties can be readily tuned through a variety of donors and acceptors.[6] Thus, in our design for low band gap chromophores, a strong electron-withdrawing heterocyclic quinoid is selected as an acceptor, namely, benzo[1,2-*c*:4,5-*c*′]bis([1,2,5]thiadiazole) (BBTD) (Figure 1). The BBTD-type unit is known to possess a substantial quinoidal character within a conjugated backbone, allowing for greater electron delocalization and thus lowering of the band gap.[7] Furthermore, the two selenium analogues, BSBT and BBSD (Figure 1), are chosen because replacement of sulfur by selenium usually leads to further band gap reduction.[7d,8] Finally, the two donors are introduced to form the D−A−D type of chromophores to facilitate a stronger intramolecular charge transfer (CT) and thus further lower the band gap energy. Although the D−A−D structure has been used to design the red- or deep red-emitting chromophores, few reports were related to the NIR-emitting compounds.[9] With these designed features, a series of NIR chromophores were synthesized and their photophysical and electrochemical properties were investigated. Furthermore, the NIR light-emitting diodes with electroluminescence above 1000 nm have been demonstrated.

(6) (a) Roncali, J. *Chem. Rev.* **1997**, *97*, 173. (b) van Mullekom, H. A. M.; Vekemans, J. A. J. M.; Havinga, E. E.; Meijer, E. W. *Mater. Sci. Eng. R* **2001**, *32*, 1. (c) Wudl, F.; Kobayashi, M.; Heeger, A. J. *J. Org. Chem.* **1984**, *49*, 3382.

(7) (a) Ono, K.; Tanaka, S.; Yamashita, Y. *Angew. Chem., Int. Ed. Engl.* **1994**, *33*, 1977. (b) Karikomi, M.; Kitamura, C.; Tanaka, S.; Yamashita, Y. *J. Am. Chem. Soc.* **1995**, *117*, 6791. (c) Kitamura, C.; Tanaka, S.; Yamashita, Y. *Chem. Mater.* **1996**, *8*, 570. (d) Yamashita, Y.; Ono, K.; Tomura, M.; Tanaka, S. *Tetrahedron* **1997**, *53*, 10169. (e) Salzner, U.; Karaltı, O.; Durdağı, S. *J. Mol. Model.* **2006**, *12*, 687. (f) Pai, C.-L.; Liu, C.-L.; Chen, W.-C.; Jenekhe, S. A. *Polymer* **2006**, *47*, 699.

(8) (a) Yang, R.; Tian, R.; Hou, Q.; Yang, W.; Cao, Y. *Macromolecules* **2003**, *36*, 7453. (b) Cao, Y.; Yang, R. Q.; Yang, W. Chinese Patent CN1389488A, 2002.

(9) (a) Velusamy, M.; Justin Thomas, K. R.; Lin, J. T.; Wen, Y. S. *Tetrahedron Lett.* **2005**, *46*, 7647. (b) Justin Thomas, K. R.; Lin, J. T.; Velusamy, M.; Tao, Y. T.; Chuen, C. H. *Adv. Funct. Mater.* **2004**, *14*, 83. (c) Kato, S.; Matsumoto, T.; Ishi, T.; Thiemann, T.; Shigeiwa, M.; Gorohmaru, H.; Maeda, S.; Yamashita, Y.; Mataka, S. *Chem. Commun.* **2004**, 2342.

Experimental Section

Materials. All chemicals and reagents were used as-received from commercial sources without purification. Solvents for chemical synthesis were purified by distillation. All chemical reactions were carried out under an argon atmosphere. 4,7-Dibromo-5,6-dinitro-2,1,3-benzothiadiazole (**10a**),[10] 4,8-dibromobenzo[1,2-*c*:4,5-*c*′]bis([1,2,5]thiadiazole) (**11a**),[7d] 4,8-dibromo[1,2,5]selenadiazolo[3,4-f]-benzo[*c*]-[1,2,5]thiadiazole (**11b**),[7d] 2-(9,9-dioctylfluoren-2-yl)thiophene (**14a**),[11] and 4-*N*,*N*-diphenylamino-1-bromobenzene (**15a**)[12] were prepared according to literature methods.

Methods. ^{1}H and ^{13}C NMR spectra were recorded using a Bruker Avance 300 NMR spectrometer (300 and 75 MHz for ^{1}H and ^{13}C, respectively). The high-temperature NMR data were obtained on a Varian Unity-400 MHz spectrometer at 373 or 403 K. Elemental analysis was performed on a Vario EL Elementar Analysis Instrument. Absorption and fluorescence spectra were recorded with Shimadzu UV-3600 spectrophotometer and PTI fluorescence system, respectively. Cyclic voltammetry was performed on a CHI660b electrochemical workstation, in dry dichloromethane containing *n*-Bu_4NPF_6 (0.1 M) with a scan rate of 50 mV/s at room temperature under argon, using a Pt disk (2 mm diameter) as the working electrode, a Pt wire as the counter electrode, and a Ag/AgCl electrode as the reference electrode. High-resolution mass spectrometry (HRMS) was obtained from Voyager-DE STR Biospectrometry and 7.0 T Actively Shielded Fourier Transform Ion Cyclotron Resonance Mass Spectrometers, respectively.

Solution emission quantum yields were performed by the method described in ref 13. A number of diluted solutions of different dye concentrations ($A < 0.1$, to prevent re-absorption) were prepared and the absorbance (A) and the integrated fluorescence intensity (D) at each concentration were recorded at given excitation wavelengths (765 nm for compounds **1**, **2**, and **M1**, 890 nm for compounds **3**−**5**, **7**, **8**, and **M2**, and 980 nm for compounds **6** and **9**). Then a graph of D versus A was plotted to determine the gradient (G). Quantum yields (Φ) were calculated using the following equation:

$$\Phi_s = \Phi_r\left(\frac{G_s}{G_r}\right)\left(\frac{I(\lambda_r)}{I(\lambda_s)}\right)\left(\frac{n_s}{n_r}\right)^2$$

The subscripts "r" and "s" refer to the reference dye and the sample, respectively. n is the refractive index of the solvent. $I(\lambda)$ is the relative intensity of the exciting light at wavelength λ. The following reference dye was used: IR-125 ($\Phi = 0.13$ in DMSO).[14]

Aggregation-Induced Emission-Enhanced (AIEE) Effect. A stock solution of **1** was prepared in THF with a concentration of 1.0×10^{-3} mol/L. Fluorescence titration was carried out by sequentially adding 1.00 mL stock solution to 99.0 mL of solvent mixtures (THF/methanol) under vigorous stirring at room temperature. The solutions were stirred for half an hour prior to taking the spectra. The fluorescence quantum yields were determined by the same method described above. IR-125 was used as a reference and the excitation wavelength for the sample was 700 nm.

OLEDs Fabrication and Measurement. The OLED was fabricated by thermal vacuum deposition on prepatterned indium tin oxide (ITO)-coated glass substrate with a sheet resistance of 10 ohms per square. The substrate was ultrasonically cleaned with acetone, detergent, deionized water, and ethanol in sequence,

(10) Uno, T.; Takagi, K.; Tomoeda, M. *Chem. Pharm. Bull.* **1980**, *28*, 1909.
(11) Belletête, M.; Beaupré, S.; Bouchard, J.; Blondin, P.; Leclerc, M.; Durocher, G. *J. Phys. Chem. B* **2000**, *104*, 9118.
(12) Li, Z. H.; Wong, M. S. *Org. Lett.* **2006**, *8*, 1499.
(13) Demas, J. N.; Crosby, G. A. *J. Phys. Chem.* **1971**, *75*, 991.
(14) Benson, R. C.; Kues, H. A. *J. Chem. Eng. Data* **1977**, *22*, 379.

followed by oxygen plasma cleaning. The thermal evaporation of organic materials was carried out at a chamber pressure of 10^{-4} Pa. The thickness of each layer was determined by a quartz thickness monitor. The effective size of the light-emitting diode was 25 mm^2. Current−voltage−power measurements were made simultaneously using a Keithley 2400 Source meter and a Newport 1830-C Optical meter equipped with a Newport 818-UV silicon photodiode, respectively. The NIR EL spectrum was measured using the PTI fluorescence spectrophotometer. All the measurements were carried out under ambient atmosphere at room temperature.

The external quantum efficiency of the NIR emission was obtained by measuring the light intensity in the forward direction and assuming the external emission profile to be Lambertian.[15] Therefore, it is possible to calculate the flux F_{ext} leaving the device directly, i.e., without being waveguided within the device. F_{ext} was calculated using the following equation:

$$F_{ext} = \int_0^{\pi/2} 2\pi L_0 \cos\theta \sin\theta \, d\theta = \pi L_0$$

where L_0 is the flux per unit solid angle of light leaving the device directly in the forward direction.

The solid angle from detector to the light source is

$$\omega = \frac{S}{l^2}$$

$$L_0 = \frac{P_{det}}{\omega}$$

Therefore, the number of photons can be calculated as follows:

$$N_p = \frac{F_{ext}}{h\nu} = \frac{\pi l^2 P_{det} \lambda}{S \cdot h \cdot c}$$

The number of electrons can be calculated from the input current as follows:

$$N_e = \frac{I}{e}$$

Thus,

$$\eta_{ext} = \frac{\pi l^2 e P_{det} \lambda}{S \cdot h \cdot c \cdot I}$$

where l is the distance between the OLED and the detector, e is the charge of an electron, P_{det} is the power that the detector measures, λ is the emission wavelength, S is the area of the detector, h is Planck's constant, c is the speed of light in vacuum, and I is the current injected.

***N*,*N*-Bis(4-octyloxyphenyl)-4-bromophenylamine (12a).** To a 250 mL round-bottomed flask equipped with a magnetic stirrer and a Dean−Stark trap under reflux condenser were added 4-bromoaniline (3.4 g, 20 mmol), 1-iodo-4-octyloxybenene (16.6 g, 50.0 mmol), cuprous iodide (0.38 g, 2.0 mmol), 1,10-phenanthroline (0.40 g, 2.0 mmol), potassium hydroxide flakes (18 g, 0.32 mol), and toluene (40 mL). The reaction mixture was rapidly heated over a period of 30 min to 125 °C and maintained at this temperature for 24 h. After cooling, the mixture was diluted with dichloromethane and washed with 1 N HCl and brine before being dried over $MgSO_4$. The crude product was purified by column chromatography (silica gel, dichloromethane/petroleum ether = 1/10) to give product (8.1 g, 70%) as colorless oil. ^{1}H NMR (300 MHz, $CDCl_3$) δ (ppm): 7.26 (d, 2H, J = 8.9 Hz), 7.05 (d, 4H, J = 8.9 Hz), 6.87−6.80 (m, 6H), 3.96 (t, 4H, J = 6.5 Hz), 1.86−1.77 (m, 4H), 1.51−1.33 (m, 20H), 0.93 (t, 6H, J = 5.1 Hz).

2-(4-(*N*,*N*-Bis(4-octyloxyphenyl)amino)phenyl)thiophene (13a). *N*,*N*-Bis(4-octyloxyphenyl)-4-bromophenylamine (**12a**) (1.5 g, 2.6 mmol), 2-(tributylstanny)thiophene (1.0 g, 2.8 mmol), and $Pd(PPh_3)_4$ (30 mg, 0.026 mmol) were charged in a 100 mL round-bottomed flask, followed by addition of 30 mL of toluene. The mixture was heated to 100 °C and maintained for 24 h. After cooling, the mixture was diluted with dichloromethane and washed with saturated aqueous potassium fluoride and brine. The separated organic layer was dried over $MgSO_4$ and the product was obtained as pale yellow oil (0.77 g, 50%) by column chromatography (silica gel, dichloromethane/petroleum ether = 1/8). ^{1}H NMR (300 MHz, $CDCl_3$) δ (ppm): 7.43 (d, 2H, J = 8.6 Hz), 7.22−7.20 (m, 2H), 7.10−7.05 (m, 5H), 6.95 (d, 2H, J = 8.3 Hz), 6.86 (d, 4H, J = 8.9 Hz), 3.96 (t, 4H, J = 6.5 Hz), 1.84−1.79 (m, 4H), 1.51−1.33 (m, 20H), 0.93 (t, 6H, J = 5.1 Hz).

2-(4-(*N*,*N*-diphenylamino)phenyl)thiophene (16a). 16a was prepared in a manner similar to that described above. Yield, 60%; pale yellow solids. ^{1}H NMR (300 MHz, $CDCl_3$) δ (ppm): 7.46 (d, 2H, J = 8.6 Hz), 7.28−7.20 (m, 6H), 7.12−7.00 (m, 9H).

General Procedure for Syntheses of Tributyltin Compounds. Tributyl[4-(*N*,*N*-bis(4-octyloxyphenyl)amino)phenyl]stannane (**12b**), tributyl[5-(4-(*N*,*N*-bis(4-octyloxyphenyl)amino)phenyl)thiophene-2-yl]stannane (**13b**), tributyl[5-(9,9-dioctylfluoren-2-yl)thiophene-2-yl]stannane (**14b**), tributyl[4-(*N*,*N*-diphenylamino)phenyl]stannane (**15b**), and tributyl[5-(4-(*N*,*N*-diphenylamino)phenyl)thiophene-2-yl]stannane (**16b**) were synthesized by a procedure similar to that described in the next paragraph.

To a solution of *N*,*N*-bis(4-octyloxyphenyl)-4-bromophenylamine (**12a**) (4.3 g, 7.4 mmol) in 20 mL of THF at −78 °C was added *n*-BuLi (2.5 M in hexane, 3.2 mL, 8.1 mmol) dropwise. After the mixture was stirred for 1.5 h, tributylstannyl chloride (2.5 mL, 8.9 mmol) was added to the mixture. Then it was slowly warmed to room temperature and stirred for another 12 h. The mixture was poured into water and extracted with diethyl ether. The organic extracts were dried over $MgSO_4$. Upon evaporation of the solvent, the crude product was obtained for the next step without further purification.

Compound 12b. Pale yellow oil. ^{1}H NMR (300 MHz, $CDCl_3$) δ (ppm): 7.26 (d, 2H, J = 8.4 Hz), 7.08 (d, 4H, J = 8.9 Hz), 6.93 (d, 2H, J = 8.4 Hz), 6.85 (d, 4H, J = 8.9 Hz), 3.96 (t, 4H, J = 6.5 Hz), 1.83−1.78 (m, 4H), 1.62−1.51 (m, 6H), 1.50−1.30 (m, 26H), 1.07−0.99 (m, 6H), 0.97−0.90 (m, 15H).

Compound 13b. Pale yellow oil. ^{1}H NMR (300 MHz, $CDCl_3$) δ (ppm): 7.45 (d, 2H, J = 8.7 Hz), 7.33 (d, 1H, J = 3.3 Hz), 7.13 (d, 1H, J = 3.3 Hz), 7.08 (d, 4H, J = 8.9 Hz), 6.95 (d, 2H, J = 8.7 Hz), 6.85 (d, 4H, J = 9.0 Hz), 3.96 (t, 4H, J = 6.5 Hz), 1.84−1.79 (m, 4H), 1.62−1.51 (m, 6H), 1.50−1.30 (m, 26H), 1.17−1.12 (m, 6H), 0.96−0.80 (m, 15H).

Compound 14b. Pale yellow oil. ^{1}H NMR (300 MHz, $CDCl_3$) δ (ppm): 7.77−7.74 (m, 2H), 7.71−7.66 (m, 2H), 7.58 (d, 1H, J = 3.3 Hz), 7.43−7.33 (m, 3H), 7.25 (d, 1H, J = 3.3 Hz), 2.10−2.07 (m, 4H), 1.73−1.68 (m, 6H), 1.49−1.42 (m, 6H), 1.26−1.13 (m, 26H), 1.03−0.98 (m, 9H), 0.90−0.86 (m, 6H), 0.80−0.60 (m, 4H).

Compound 15b. Pale yellow oil. ^{1}H NMR (300 MHz, $CDCl_3$) δ (ppm): 7.30 (d, 2H, J = 7.5 Hz), 7.26−7.21 (m, 4H), 7.10−6.97 (m, 8H), 1.59−1.48 (m, 6H), 1.35−1.28 (m, 6H), 1.04−0.99 (m, 6H), 0.91−0.86 (m, 9H).

Compound 16b. Brown oil. ^{1}H NMR (300 MHz, $CDCl_3$) δ (ppm): 7.49 (d, 2H, J = 8.5 Hz), 7.34 (d, 1H, J = 3.3 Hz), 7.28−7.22 (m, 4H), 7.12−7.00 (m, 9H), 1.64−1.56 (m, 6H), 1.39−1.31 (m, 6H), 1.14−1.09 (m, 6H), 0.94−0.88 (m, 9H).

(15) Greenham, N. C.; Friend, R. H.; Bradley, D. D. C. *Adv. Mater.* **1994**, *6*, 491.

4,8-Bis[4-(*N*,*N*-diphenylamino)phenyl]benzo[1,2-*c*:4,5-*c*′]bis([1,2,5]thiadiazole) (M1). To a solution of compounds **15b** (1.3 g, 2.4 mmol) and **11a** (0.35 g, 1.0 mmol) in toluene (100 mL) was added $Pd(PPh_3)_4$ (46 mg, 0.040 mmol). The mixture was stirred for 48 h at 100 °C. After workup, the solvent was evaporated under vacuum and the residue was washed by ethanol to give a green solid (0.52 g). The product was further purified by vacuum sublimation twice before characterization to afford a green solid (0.28 g, 41%). ^{1}H NMR (400 MHz, $C_2D_2Cl_4$, 373K) δ (ppm): 8.28 (d, 4H, J = 7.2 Hz), 7.33−7.29 (m, 8H), 7.26−7.22 (m, 12H), 7.11 (t, 4H, J = 6.0 Hz). Anal. Calcd for $C_{42}H_{28}N_6S_2$: C, 74.09; H, 4.15; N, 12.34. Found: C, 73.79; H, 3.89; N, 12.18. HRMS: calcd, 680.18169; found, 680.17865.

4,8-Bis(5-(4-(*N*,*N*-diphenylamino)phenyl)-2-thiophene)benzo[1,2-*c*:4,5-*c*′]bis([1,2,5] thiadiazole (M2). M2 was prepared in a manner similar to that described above. Yield: 45%; black solids. ^{1}H NMR (400 MHz, $C_2D_2Cl_4$) δ (ppm): 8.97 (br, 2H), 7.60 (br, 4H), 7.43 (br, 2H), 7.26−7.24 (m, 8H), 7.13−7.06 (m, 16H). Anal. Calcd for $C_{50}H_{32}N_6S_4$: C, 71.06; H, 3.82; N, 9.94. Found: C, 71.32; H, 3.73; N, 10.04. HRMS: calcd, 844.15713; found, 844.15591.

4,8-Bis[4-(*N*,*N*-bis(4-octyloxyphenyl)amino)phenyl]benzo[1,2-*c*:4,5-*c*′]bis([1,2,5]thiadiazole) (1). To a solution of compounds **12b** (1.2 g, 1.5 mmol) and **11a** (0.19 g, 0.54 mmol) in toluene (40 mL) was added $Pd(PPh_3)_4$ (71 mg, 0.061 mmol). The mixture was stirred for 36 h at 100 °C. After cooling to room temperature, the mixture was poured into water and extracted with dichloromethane. The organic layer was washed with saturated aqueous potassium fluoride and brine before being dried over $MgSO_4$. After evaporation of the solvent, the residue was purified by column chromatography on silica gel with dichloromethane:petroleum ether (1:1) as the eluent to afford product (0.21 g, 33%) as green solids. ^{1}H NMR (300 MHz, $CDCl_3$) δ (ppm): 8.17 (d, 4H, J = 8.1 Hz), 7.26−7.00 (m, 12H), 6.89 (d, 8H, J = 7.8 Hz), 3.98 (t, 8H, J = 6.3 Hz), 1.86−1.76 (m, 8H), 1.57−1.32 (m, 40H), 0.91 (t, 12H, J = 6.3 Hz). ^{13}C NMR (75 MHz, $CDCl_3$) δ (ppm): 156.46, 153.13, 140.32, 132.96, 127.92, 120.45, 119.01, 115.76, 68.68, 32.22, 29.77, 29.65, 26.49, 23.06, 14.50. Anal. Calcd for $C_{74}H_{92}N_6O_4S_2$: C, 74.46; H, 7.77; N, 7.04. Found: C, 73.47; H, 7.63; N, 6.57. HRMS: calcd, 1192.6622; found, 1192.7015.

4,8-Bis(4-(*N*,*N*-bis(4-octyloxyphenyl)amino)phenyl)[1,2,5]selenadiazolo[3,4-*f*]benzo[*c*][1,2,5]-thiadiazole (2). It was synthesized according to the same procedure as that used in the preparation of **1**. Yield, 40%; green solids. ^{1}H NMR (300 MHz, $CDCl_3$) δ (ppm): 8.02 (d, 4H, J = 8.1 Hz), 7.17 (br, 12H), 6.86 (d, 8H, J = 8.0 Hz), 3.94 (t, 8H, J = 6.3 Hz), 1.80−1.73 (m, 8H), 1.46−1.29 (m, 40H), 0.90−0.86 (m, 12H). ^{13}C NMR (75 MHz, $CDCl_3$) δ (ppm): 156.46, 153.29, 140.34, 133.21, 127.89, 118.92, 115.75, 68.68, 32.22, 29.77, 29.65, 26.49, 23.06, 14.50. Anal. Calcd for $C_{74}H_{92}N_6O_4SSe$: C, 71.64; H, 7.47; N, 6.77. Found: C, 70.42; H, 7.77; N, 5.97. HRMS: calcd, 1240.60660; found, 1240.60676.

4,8-Bis(5-(9,9-Dioctylfluoren-2-yl)-2-thiophene)benzo[1,2-*c*:4,5-*c*′]bis([1,2,5]thiadiazole) (4). Yield, 62%; green solids. ^{1}H NMR (400 MHz, $C_2D_2Cl_4$) δ (ppm): 9.03 (br, 2H), 7.74−7.72 (m, 8H), 7.60 (br, 2H), 7.36−7.32 (m, 6H), 2.04 (br, 8H), 1.19−1.10 (m, 40H), 0.80−0.79 (m, 20H). ^{13}C NMR (75 MHz, $CDCl_3$) δ (ppm): 152.00, 151.44, 150.37, 141.83, 141.05, 139.43, 137.65, 134.37, 133.35, 127.71, 127.29, 125.38, 124.51, 123.33, 120.58, 120.27, 113.41, 55.72, 40.92, 32.20, 30.52, 29.66, 24.29, 22.99, 14.46. Anal. Calcd for $C_{72}H_{86}N_4S_4$: C, 76.14; H, 7.63; N, 4.93. Found: C, 75.64; H, 7.21; N, 4.74. HRMS: calcd, 1134.5735; found, 1135.7426.

4,8-Bis(5-(9,9-dioctylfluoren-2-yl)-2-thiophene)[1,2,5]selenadiazolo[3,4-*f*]benzo[*c*][1,2,5]thiadiazole (5). Yield, 59%; black solids. ^{1}H NMR (300 MHz, $CDCl_3$) δ (ppm): 8.90 (br, 2H), 7.74 (br, 8H), 7.53 (br, 2H), 7.38−7.36 (m, 6H), 2.10−2.08 (m, 8H), 1.20−1.10 (m, 40H), 0.82−0.77 (m, 20H). ^{13}C NMR (75 MHz, $CDCl_3$) δ (ppm): 156.79, 151.63, 151.23, 151.05, 150.43, 141.44, 140.69, 138.47, 134.57, 133.17, 127.31, 126.91, 124.96, 124.24, 122.95, 120.20, 120.00, 119.87, 113.06, 55.33, 40.54, 31.81, 30.14, 29.32, 29.27, 23.91, 22.60, 14.07. HRMS: calcd, 1182.51798; found, 1182.47231.

4,8-Bis(5-(4-(*N*,*N*-bis(4-octyloxyphenyl)amino)phenyl)-2-thiophene)benzo[1,2-*c*:4,5-*c*′]bis([1,2,5]thiadiazole) (7). Yield, 35%; black solids. ^{1}H NMR (400 MHz, *o*-$C_6D_4Cl_2$, 403 K) δ (ppm): 9.08 (br, 2H), 7.65 (br, 4H), 7.46 (br, 2H), 7.17 (d, 8H, J = 7.6 Hz), 7.04 (d, 4H, J = 7.2 Hz), 6.92 (d, 8H, J = 8.0 Hz), 3.98 (t, 8H, J = 6.0 Hz), 1.82−1.79 (m, 8H), 1.50−1.49 (m, 8H), 1.34−1.32 (m, 32H), 0.92−0.90 (m, 12H). ^{13}C NMR (75 MHz, *o*-$C_6D_4Cl_2$) δ (ppm): 157.09, 151.86, 149.93, 141.01, 137.80, 132.93, 128.27, 123.72, 120.71, 116.40, 113.61, 69.10, 32.94, 30.56, 30.44, 27.27, 23.81, 15.14. Anal. Calcd for $C_{82}H_{96}N_6O_4S_4$: C, 72.53; H, 7.13; N, 6.19. Found: C, 72.27; H, 6.66; N, 6.24. HRMS: Calcd, 1356.63759; found, 1356.62386.

4,8-Bis(5-(4-(*N*,*N*-bis(4-octyloxyphenyl)amino)phenyl)-2-thiophene)[1,2,5]selenadiazolo[3,4-*f*]benzo[*c*][1,2,5]thiadiazole (8). Yield, 40%; black solids. ^{1}H NMR (400 MHz, *o*-$C_6D_4Cl_2$, 403 K) δ (ppm): 9.03 (br, 2H), 7.66 (br, 4H), 7.46 (br, 2H), 7.17 (d, 8H, J = 6.8 Hz), 7.04 (d, 4H, J = 6.8 Hz), 6.92 (d, 8H, J = 8.0 Hz), 3.98 (t, 8H, J = 6.4 Hz), 1.84−1.77 (m, 8H), 1.50−1.48 (m, 8H), 1.34−1.28 (m, 32H), 0.91−0.90 (m, 12H). Anal. Calcd for $C_{82}H_{96}N_6O_4S_3Se$: C, 70.11; H, 6.89; N, 5.98. Found: C, 69.40; H, 6.94; N, 5.35. HRMS: Calcd, 1404.58204; found, 1404.57151.

Dinitro Compound 10b. To a solution of 4,7-dibromo-5,6-dinitro-2,1,3-benzothiadiazole (**10a**) (1.2 g, 3.2 mmol) and tributyl[4-(*N*,*N*-bis(4-octyloxyphenyl)amino)phenyl]stannane (**12b**) (5.6 g, 7.1 mmol) in toluene (80 mL) was added $Pd(PPh_3)_4$ (46 mg, 0.039 mmol) under an argon atmosphere. The mixture was stirred for 36 h at 100 °C. After cooling to room temperature, the mixture was poured into water and extracted with dichloromethane. The organic layer was washed with saturated aqueous potassium fluoride and brine before being dried over $MgSO_4$. After evaporation of the solvent, the residue was purified by column chromatography on silica gel with dichloromethane:petroleum ether (1:1) as the eluent to afford product (3.4 g, 87%) as purple solids. ^{1}H NMR (300 MHz, $CDCl_3$) δ (ppm): 7.38 (d, 4H, J = 8.8 Hz), 7.19 (d, 8H, J = 8.7 Hz), 6.98 (d, 4H, J = 8.7 Hz), 6.91 (d, 8H, J = 8.9 Hz), 3.98 (t, 8H, J = 6.5 Hz), 1.87−1.77 (m, 8H), 1.50−1.33 (m, 40H), 0.98−0.90 (m, 12H).

10c. Dark blue solids; 60% yield. ^{1}H NMR (300 MHz, $CDCl_3$) δ (ppm): 7.47−7.43 (m, 6H), 7.25−7.24 (m, 2H), 7.07 (d, 8H, J = 8.7 Hz), 6.90 (d, 4H, J = 8.5 Hz), 6.83 (d, 8H, J = 8.9 Hz), 3.93 (t, 8H, J = 6.3 Hz), 1.82−1.73 (m, 8H), 1.47−1.28 (m, 40H), 0.82 (t, 12H, J = 6.3 Hz).

10d. Mauve solids; 80% yield. ^{1}H NMR (300 MHz, $CDCl_3$) δ (ppm): 7.75−7.62 (m, 8H), 7.54 (d, 2H, J = 4.0 Hz), 7.48 (d, 2H, J = 4.0 Hz), 7.38−7.30 (m, 6H), 2.03−1.98 (m, 8H), 1.19−1.05 (m, 40H), 0.79 (t, 12H, J = 6.6 Hz), 0.64−0.62 (m, 8H).

4,8-Bis(4-(*N*,*N*-bis(4-octyloxyphenyl)amino)phenyl)benzo[1,2-*c*:4,5-*c*′]bis([1,2,5]selenadiazole) (3). To a suspension of compound **10b** (0.51 g, 0.42 mmol) in acetic acid (50 mL) was added zinc powder (0.55 g, 8.4 mmol). The mixture was stirred at 60 °C for 3 h until the color of the reaction mixture turned white. After cooling to room temperature, a large amount of water was added and precipitates were filtrated and dried under vacuum. The isolated tetraamine compound was, without further purification, reacted with selenium dioxide (0.23 g, 2.1 mmol) in freshly distilled dichloromethane (50 mL) at room temperature for 6 h. After removal of the solvent under reduced pressure, the residue was purified by

Scheme 1. Synthetic Route to Intermediates and Chromophores 1−9

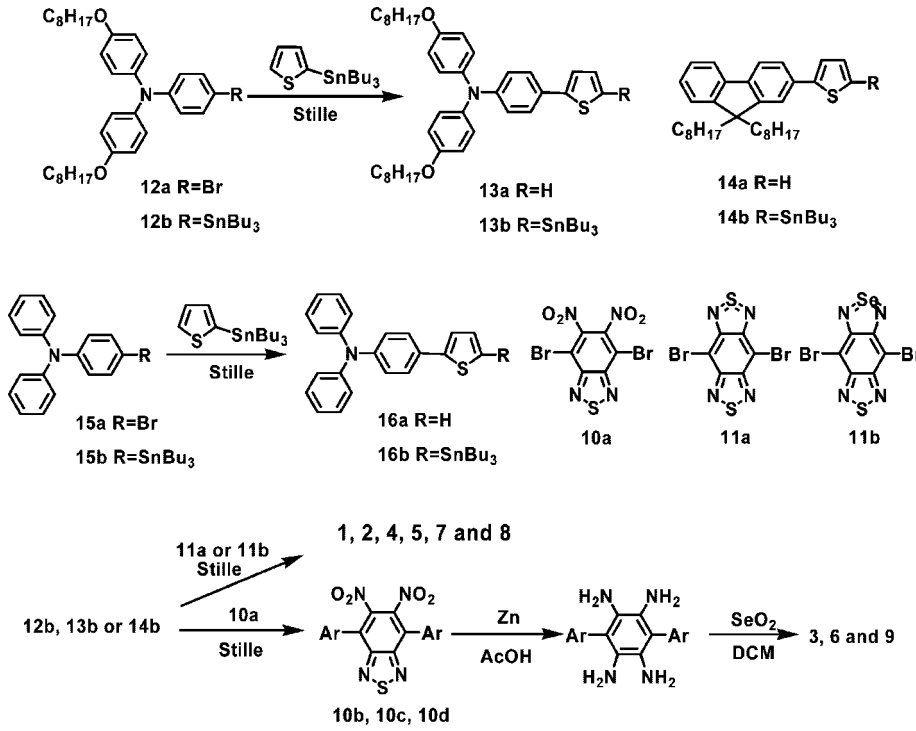

column chromatography on neutral Al_2O_3 (eluent dichloromethane/petroleum ether = 1/2 v/v) to give compound **3** (108 mg, 20%) as gray solids. ^{1}H NMR (300 MHz, $CDCl_3$) δ (ppm): 7.95 (d, 4H, J = 7.7 Hz), 7.17−7.08 (m, 12 H), 6.85 (d, 8H, J = 8.4 Hz), 3.94 (t, 8H, J = 6.3 Hz), 1.82−1.73 (m, 8H), 1.45−1.28 (m, 40H), 0.88 (t, 12H, J = 6.3 Hz). HRMS: Calcd, 1288.55105; found, 1288.55178.

4,8-Bis(5-(9,9-dioctylfluoren-2-yl)-2-thiophene)benzo[1,2-*c*:4,5-*c*′]bis([1,2,5]selenadiazole) (6). According to the procedure for the preparation of **3**, compound **6** was synthesized from the dinitro compound **10d.** Yield, 30%; black solids. ^{1}H NMR (300 MHz, $CDCl_3$) δ (ppm): 9.04 (br, 2H), 7.73 (m, 8H), 7.59 (d, 2H, J = 3.4 Hz), 7.36 (m, 6H), 2.07 (m, 8H), 1.24−1.08 (m, 40H), 0.87−0.68 (m, 20H). ^{13}C NMR (75 MHz, $CDCl_3$) δ (ppm): 150.58, 150.03, 140.45, 139.65, 132.23, 126.30, 125.88, 123.94, 123.69, 121.91, 119.14, 118.85, 54.30, 39.52, 30.78, 29.11, 28.29, 28.24, 22.89, 21.57, 13.04. Anal. Calcd for $C_{72}H_{86}N_4S_2Se_2$: C, 70.33; H, 7.05; N, 4.56. Found: C, 69.33; H, 6.94; N, 4.16. HRMS: Calcd, 1230.46243; found, 1230.45616.

4,8-Bis(5-(4-(*N*,*N*-bis(4-octyloxyphenyl)amino)phenyl)-2-thiophene)benzo[1,2-*c*:4,5-*c*′]bis([1,2,5]selenadiazole) (9). According to the procedure for the preparation of **3**, compound **9** was synthesized from compound **10c**. Yield, 17%; black solids. ^{1}H NMR (400 MHz, *o*-$C_6D_4Cl_2$, 403 K) δ (ppm): 8.26 (s, 2H), 7.54 (br, 4H), 7.42−7.40 (m, 2H), 7.16−7.13 (m, 8H), 7.07 (d, 4H, J = 6.4 Hz), 6.93 (d, 8H, J = 6.4 Hz), 3.98 (br, 8H), 1.93−1.80 (m, 8H), 1.50−1.32 (m, 40H), 0.91 (br, 12H). HRMS: Calcd, 1452.52649; found, 1452.51697.

Results and Discussion

Design and Synthesis. The design concept and chemical structures of the new D−A−D chromophores (**1**−**9**) are illustrated in Figure 1. Schemes 1 and 2 outline the synthetic routes to a series of nine compounds plus two chromophores **M1** and **M2**. Compounds **1**−**9** are designed mainly for the purpose of the study of the structure−property relationships and therefore contain long aliphatic groups that can impart

Scheme 2. Synthetic Route to Chromophores M1 **and** M2

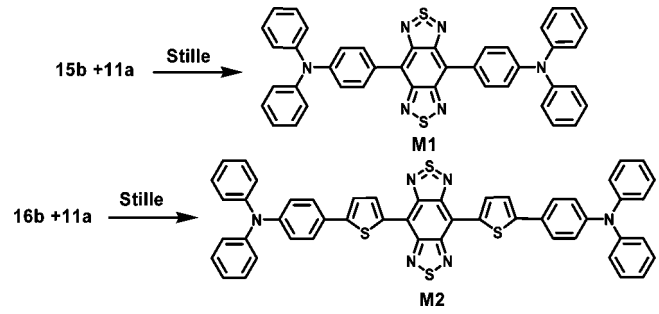

the solubility to the chromophores. Compounds **M1** and **M2** are structurally related to **1** and **7**, respectively, and therefore should have band gaps similar to those of **1** and **7**. Without long aliphatic chains, they should be readily sublimed and thus can be used in the LED by vapor deposition for a purpose of demonstration of the NIR OLEDs in this work. The BBTD- and BSBT-based chromophores were readily synthesized by the Stille-coupling reaction of dibromo-BBTD and dibromo-BSBT with the tributyltin compounds derived from the corresponding donors, respectively. The BBSD-based chromophores (**3**, **6**, **9**) were obtained by the Stille-coupling reaction of 4,7-dibromo-5,6-dinitrobenzo[*c*][1,2,5]-thiadiazole with the corresponding donors, followed by complete reduction of the nitro groups and thiadiazole and subsequent cyclization with selenium dioxide. Compounds **1**−**9** are soluble in common organic solvents such as chloroform, THF, and toluene, whereas **M1** and **M2** sublime at elevated temperatures under vacuum.

Optical Properties. The absorption and photoluminescence of compounds **1**−**9** were recorded in toluene (Figure 2) and the data were presented in Table 1. The absorption bands in the region from 300 to 600 nm are attributed to $\pi-\pi^*$ and n−π^* transitions of the conjugated aromatic

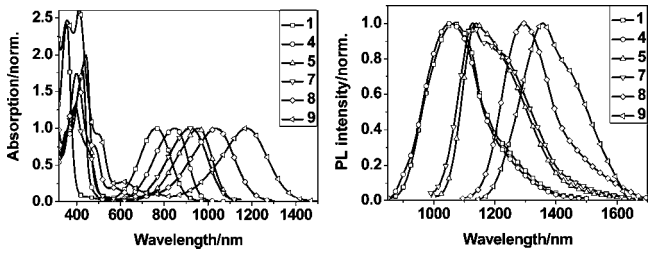

Figure 2. Normalized absorption (left, 1×10^{-5} M) and fluorescence emission (right, 1×10^{-4} M) spectra of chromophores **1**−**9** in toluene.

segments, and those at longer wavelengths are due to the intramolecular CT transitions between the peripheral donor groups and the acceptor cores. Their absorption bands at 600−1400 nm are well-separated from higher energy bands, indicating a strong CT character of these D−A−D chromophores.[16] An anticipated bathochromic shift was observed by increasing the donor strength, e.g., from the fluorene to triphenylamine (TPA) donor (93 nm red shift from **6** to **9**). Incorporation of a thiophene bridging unit resulted in a larger bathochromic shift (e.g., 245 nm from **3** to **9**), due to extended conjugation length and enhanced intramolecular charge transfer. When the sulfur atom in acceptor cores is replaced by selenium atom, such as the BSBT and BBSD, an even larger red shift in absorption is induced (e.g., 141 nm for **9** vs **8**). Nearly the same trend in the structure−PL property relationship for chromophores **1**−**9** was also observed (Figure 2, Table 1). It is worth noting that compound **9** absorbs at the longest wavelength ($\lambda_{max} = 1177$ nm) and its PL falls in the telecommunication band region (e.g., 1300−1550 nm). Its emission peak shifts gradually from 1335 to 1480 nm with the increase in concentration from 10^{-5} to 10^{-3} mol/L (Figure 3). Since its absorption remains unchanged with different concentrations, **9** readily forms the excimer in toluene.[17] As expected, compounds **1**−**9** are solvatochromic (Table 2), which further confirms the presence of a strong intramolecular CT in these compounds. The emission spectra of compounds show a positive solvatochromism, indicating that the dipole moment is larger in the excited state than in the ground state.[18] The fluorescence quantum efficiency is quite high, compared to those of the other NIR dyes, though it is well-known that the emission efficiency in the D−A system is usually low.[19] It should be noted that among all, compound **4** has a quite high fluorescence quantum efficiency of 18.5%, due to its more rigid fluorene structure.

The highly fluorescent NIR dyes in the solid state are desirable for various applications. After quick screening, **1** was found to exhibit an aggregation-induced emission enhancement (AIEE) effect and emit strongly at 1078 nm in the solid state (Figure 4a). By adding a nonsolvent (methanol) to the THF solution of **1**, the originally rather weak PL increased significantly. The PL quantum yields (Φ_F) of **1** remained almost constant at about 0.1% before reaching 70% methanol in THF and increased to 2.9% at 90% methanol−THF (Figure 4b). Without the apparent light scattering in measurement, the actual Φ_F of the aggregates or solid film of **1** could be even higher. The calculation on the optimized geometry shows that **1** has a more twisted conformation because of the TPA moiety than others (e.g., **4**). The AIEE phenomenon in **1** is believed to originate from the suppressed chromophore aggregation and restricted intramolecular vibrational and rotational motions in the solid state.

In comparison, the thin film of **M1**, made by vacuum sublimation, absorbs at 723 nm and emits at 1050 nm (Figure 7a), similar to compound **1** ($\lambda_{max}^{abs} = 754$ nm and $\lambda_{max}^{PL} = 1078$ nm in film). **M2** is structurally related to compound **7** ($\lambda_{max}^{abs} = 920$ nm and $\lambda_{max}^{PL} = 1125$ m in toluene) and absorbs at 879 nm and emits at 1120 nm in toluene.

Electrochemical Properties. The electrochemical properties of compounds **1**−**9** are investigated by cyclic voltammetry (CV) (Figure 5) and the data are summarized in Table 3. They are all electrochemically active, having two or three quasi-reversible reduction waves in cyclic voltammogram. The first reduction potentials in a range from −0.8 to −1.2 V (relative to ferrocene) are from the reduction of acceptor cores. The reversible oxidation waves were also observed and the first one could be attributed to the oxidation of the donors such as the TPA moiety in **1** ($E_{1/2} = 0.17$ V). However, unlike compound **1**, compound **7** shows two reversible oxidation processes at $E_{ox}^1 = -0.04$ V and $E_{ox}^2 = 0.11$V, respectively, which means that the two electrons are removed successively from the two nitrogen centers. Because of the strong electron-donating strength of TPA, the first oxidation wave was at a lower potential (e.g., 0.33 V for **4** vs −0.04 V for **7**). The HOMO, LUMO, and band gap levels of compounds **1**−**9** were obtained from their electrochemical data, which coincide well with the values from theoretic calculations (Table 1). The selenium analogues show lower band gap, presumably due to more hybridization of energy levels of donor and acceptor fragment with a large selenium atom. Among all, compound **9** has the lowest band gap of 0.56 eV. The electrochemical properties of **M1** and **M2** were also studied and their band gaps (1.27 V for **M1** and 0.98 V for **M2**) were found to be similar to those of compounds **1** and **7**.

Computational Studies. The optimized geometries of three compounds (**1**, **4**, and **7**) are calculated by using the Amsterdam Density Functional program package (ADF 2006.1b)[20] at the level of gradient corrected density functional theory with the Becke-Perdew exchange correlation functional.[21] To minimize computational effort, the solubilizing alkyl and alkoxy substituents were replaced by hydrogen. The molecules' geometries were optimized without any symmetry and geometry constraints. A standard double

(16) Amthor, S.; Lambert, C.; Dümmler, S.; Fischer, I.; Schelter, J. *J. Phys. Chem. A* **2006**, *110*, 5204.
(17) Halkyard, C. E.; Rampey, M. E.; Kloppenburg, L.; Studer-Martinez, S. L.; Bunz, U. H. F. *Macromolecules* **1998**, *31*, 8655.
(18) Reichardt, C. *Chem. Rev.* **1994**, *94*, 2319.
(19) Brédas, J. L.; Cornil, J.; Beljonne, D.; dos Santos, D. A.; Shuai, Z. *Acc. Chem. Res.* **1999**, *32*, 267.
(20) (a) ADF2006.01, SCM, Theoretical Chemistry, Vrije Universiteit, Amsterdam, The Netherlands, http://www.scm.com. (b) te Velde, G.; Bickelhaupt, F. M.; van Gisbergen, S. J. A.; Fonseca Guerra, C.; Baerends, E. J.; Snijders, J. G.; Ziegler, T. *J. Comput. Chem.* **2001**, *22*, 931. (c) Fonseca Guerra, C.; Snijders, J. G.; te Velde, G.; Baerends, E. J. *Theor. Chem. Acc.* **1998**, *99*, 391.
(21) (a) Becke, A. *Phys. Rev. A* **1988**, *38*, 3098. (b) Perdew, J. P. *Phys. Rev. B* **1986**, *34*, 7406. (c) Perdew, J. P. *Phys. Rev. B* **1986**, *33*, 8822.

Table 1. Optical and Electrochemical Data of Chromophores

chromophore	λ_{max}^{abs} [nm][a]	Δ_{abs} [nm]	Log ε[a]	λ_{max}^{PL} [nm][b]	Stokes shift [nm]	Φ_f [%][c]	HOMO (eV)[d]	LUMO (eV)[d]	band gap (eV)[e]
1	763		4.38	1065	302	7.1	4.95	3.76	1.19 (1.04)
2	837	74	4.45	1120	283	2.8	4.95	3.82	1.13 (0.91)
3	932	95	4.04	1230	298	1.8	4.89	3.95	0.94 (0.83)
4	848		4.71	1055	207	18.5	5.14	3.99	1.15 (1.04)
5	954	106	4.56	1120	166	4.6	5.01	4.08	0.93 (0.90)
6	1084	130	4.48	1285	201	1.9	4.96	4.14	0.82 (0.66)
7	920		4.86	1125	205	5.3	4.77	3.94	0.83 (0.87)
8	1036	116	4.48	1295	259	1.1	4.66	4.02	0.64 (0.78)
9	1177	141	4.17	1360	183	<1	4.68	4.12	0.56 (0.61)
M1	709		4.14	975	266	7.4	5.15	3.88	1.27
M2	879		4.52	1120	241	4.9	4.95	3.97	0.98

[a] Measured in toluene with a concentration of 1×10^{-5} M. [b] Measured in toluene with a concentration of 1×10^{-4} M. Excitation wavelengths for **1**−**5**, **7**, **M1**, and **M2** are at their maximum absorption wavelengths; for **6**, **8**, and **9** they are at 980 nm. [c] Fluorescence quantum yield measured relative to IR-125 ($\Phi_f = 0.13$ in DMSO). [d] Calculated from the formula, $E_{(HOMO)} = -(E_{ox} + 4.34)$ (eV), $E_{(LUMO)} = -(E_{red} + 4.34)$ (eV). [e] Calculated values are in the parentheses as obtained.

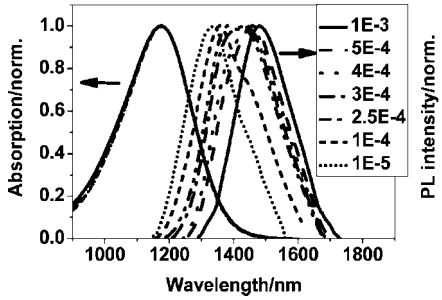

Figure 3. Absorption and PL spectra of **9** in toluene with different concentrations.

Table 2. Wavelengths (nm) of Maximal PL of Some Chromophores in Different Solvents (1×10^{-4} M)

chromophore	hexane	toluene	CH_2Cl_2	DMF
1	1000	1065	1125	1130
4	1025	1055	1090	1110
5	1120	1120	1205	1145
7	1105	1125	1255	
8	1265	1295	1330	
9		1360	1485	

STO basis set with polarization function (DZP) was employed for all atoms. The frozen core approximation was employed for the 1s electrons of the C, O, and N atoms, up to and including the 2p electrons of sulfur and the 3d electrons of selenium. Numerical integrations were performed with the integration precision of 4.0, and the default ADF values were chosen for the self-consistent-field (SCF) and geometry optimization convergence criteria. The optimized geometries are shown in Figure 6 and some dihedral parameters are listed in Table 4. The calculation clearly reveals that although the benzobis(thiadiazole) moiety is

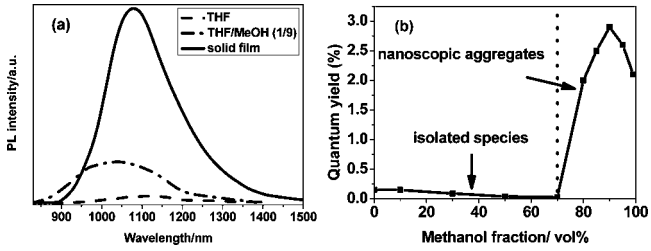

Figure 4. (a) PL spectra of **1** in THF/methanol (1:9 v/v) and THF and as a film; concentration of **1**, 10 μM; excitation wavelength (nm), 700 (for solution), 694 (for film). (b) Quantum yield of **1** vs solvent composition of the THF/methanol mixture.

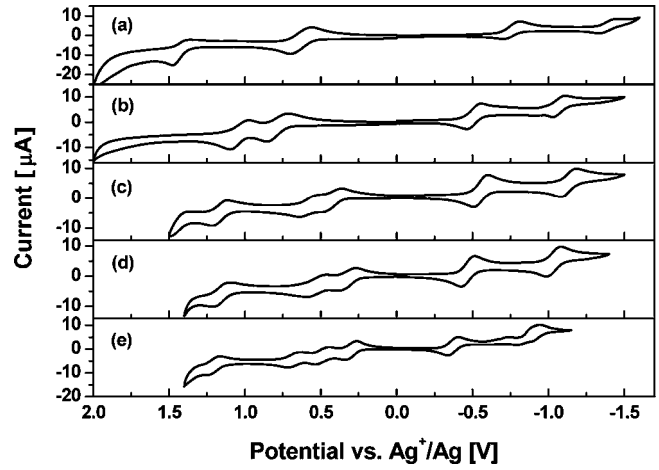

Figure 5. Cyclic voltammograms of compounds **1** (a), **4** (b), **7** (c), **8** (d), and **9** (e) in dichloromethane.

Table 3. CV Data of Compounds 1−9[a]

compd	E_{ox}^1 (V)	E_{ox}^2 (V)	E_{ox}^3 (V)	E_{ox}^4 (V)	E_{red}^1 (V)	E_{red}^2 (V)	E_{red}^3 (V)
1	+0.17	+0.96			−1.22	−1.86	
2	+0.14	+1.06			−1.12	−1.91	
3	+0.06	+0.26	+0.93		−1.02	−1.23	−1.71
4	+0.33	+0.58			−0.98	−1.53	
5	+0.26	+0.53			−0.85	−1.39	
6	+0.15	+0.45			−0.81	−1.35	
7	−0.04	+0.11	+0.70		−1.02	−1.60	
8	−0.14	+0.06	+0.69		−0.93	−1.50	
9	−0.16	+0.02	+0.21	+0.74	−0.85	−1.32	−1.39

[a] E is in units of volts with reference to ferrocene.

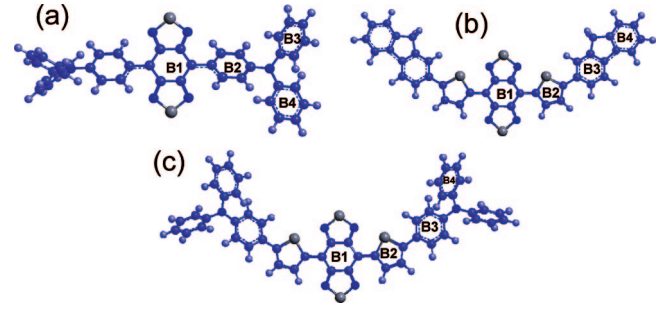

Figure 6. The optimized geometries of **1** (a), **4** (b), and **7** (c).

planar, the linked two phenyl groups are twisted with a dihedral angle of 41.8°. Thus, with the twisted TPA, compound **1** has a totally nonplanar structure. This kind of molecular configuration can effectively prevent the $\pi-\pi$ interaction in the solid state and suppress the concentration-

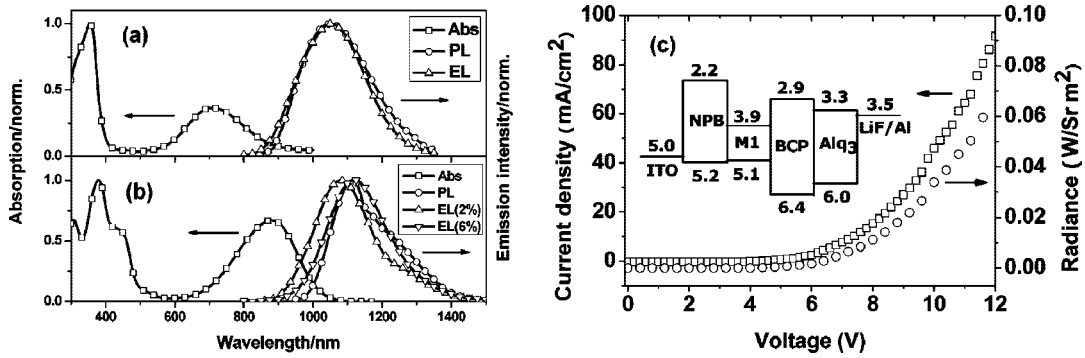

Figure 7. (a) Absorption (film), PL (film), and EL spectra of **M1**. (b) Absorption (in toluene), PL (in toluene), and EL spectra of **M2**. (c) Current density−voltage−radiance characteristics of LED and the proposed energy level scheme (inset) of **M1**.

Table 4. Dihedral Angles of 1, 4, **and** 7

dihedral angles	**1** [deg]	**4** [deg]	**7** [deg]
B1−B2	41.82	0.02	5.39
B2−B3	43.46	18.29	8.77
B3−B4	41.70	0.29	39.79

induced PL quenching. Compound **7**, although also containing TPA, has relatively smaller dihedral angles between thiophene and BBTD (B1/B2), thiophene and phenyl (B2/B3), and thus is basically planar. Compound **4** is even more planar than **7** and therefore its fluorescence is largely quenched in the solid state.

Electroluminescent Property. To demonstrate the potential of this class of chromophores as an NIR emitter, LEDs with two different configurations were fabricated: ITO/PEDOT:PSS/emissive layer/Al and ITO/MoO_3/NPB/emissive layer/BCP/Alq_3/LiF/Al. The former is a simple device and suitable for the solution-processable chromophores such as compounds **1**−**9**; the latter is the multilayered device and requires the use of materials which could be sublimed. Limited by the device simplicity and poor quality film of emissive layer made by spin-coating of the small molecules, the LEDs with the simple one-layer configuration, based on soluble chromophores (e.g., **1**−**9**), emitted rather weak NIR light and the EL EQE was too low to be calculated.

With use of compound **M1**, the LED device was designed with a proposed energy level scheme shown in Figure 7c (inset) and fabricated with a configuration of ITO/MoO_3(8 nm)/NPB(40 nm)/**M1**(20 nm)/BCP(10 nm)/Alq_3(30 nm)/LiF(1 nm)/Al. NPB and Alq_3 were used as holes and electron-transporting layers, respectively. BCP was chosen to block the hole and eliminate the visible emission from Alq_3. Because of the low injection barrier (ca. 0.2 eV), the turn-on voltages were under 5 V. This all-organic device emitted the eye-invisible light with a maximal EL peak at 1050 nm (Figure 7a) and the maximal radiance of 60 mW/Sr·m^2 (Figure 7c). A good match between the EL and PL spectra of **M1** indicates the observed EL solely from the emitter **M1**. Without further optimization, the EQE of the current device reached 0.05%. To probe the effect of the electron mobility on the EL quantum yield, another device with a configuration of ITO/MoO_3(8 nm)/NPB(40 nm)/**M1**(20 nm)/TPBI(40 nm)/LiF(1 nm)/Al was made. The LUMO level of TPBI (2.7 eV) is higher than that of Alq_3 (3.3 eV); the electron injection in this device should be more difficult. Indeed, the device resulted in a lower EL quantum yield and therefore the device efficiency based on such a D−A−D chromophore system is governed by the electron injection or mobility.

Modification of the device configuration by adjusting the thickness and composition (e.g., use of a host) of the emitting layer is likely to increase the EQE. Therefore, another LED device was fabricated using **M2** as a dopant in the emissive layer. Specifically, **M2** was co-evaporated with Alq_3 to form the emissive layer in the LEDs with a configuration of ITO/MoO_3(8 nm)/NPB(50 nm)/Alq_3:**M2**(*x* wt %, 30 nm)/BAlq(15 nm)/LiF(1 nm)/Al. BAlq was used as an electron-transporting and a hole-blocking layer. Figure 7b shows the EL spectra of the devices with a different dopant concentration (2% and 6%). At 2% doping, due to the inefficient energy transfer or charge trapping, the spectrum displays two EL peaks from Alq_3 at 530 nm and from **M2** at 1085 nm, respectively (the visible EL was not shown in Figure 7b). When the doping concentration was adjusted to 6%, the visible emission disappeared completely and the spectrum displayed exclusive NIR emission at 1115 nm. It was also found that the EL spectra were red-shifted about 30 nm as the concentration increased from 2 to 6%, which could be attributed to a strong polarization effect as seen often in many red dopant systems.[22] The EQE of the OLED (6% **M2**) is not available because its emission extends into the spectral region in which currently available Si detector is not sensitive. Our preliminary studies on the LED devices clearly indicate that both the properties of chromophores and device configuration are critically important for realization of NIR OLEDs.

Conclusion

A series of soluble, fluorescent compounds with the PL ranging from 900 to 1600 nm are obtained and their optophysical and electrochemical properties are studied. This work shows that a combination of TPA, thiophene, and BBSD in the D−A−D system can lead to the longest emission wavelength and the narrowest band gap (e.g., **9**).

(22) (a) Tang, C. W.; VanSlyke, S. A.; Chen, C. H. *J. Appl. Phys.* **1989**, *65*, 3610. (b) Bulovič, V.; Shoustikov, A.; Baldo, M. A.; Bose, E.; Kozlov, V. G.; Thompson, M. E.; Forrest, S. R. *Chem. Phys. Lett.* **1998**, *287*, 455.

The maximum emission wavelength of **9** is also concentration-dependent and could reach 1480 nm, which is the longest for organic compounds without rare earth metal ions. The all-organic LED device with exclusive NIR emission at 1050 nm has been realized. By doping, the emission wavelength can be extended up to 1115 nm, demonstrating a great potential of heteroquinoid-based D−A−D chromophores as NIR light-emitting materials for further technological innovations.

Acknowledgment. This work was supported by the Changchun Institute of Applied Chemistry and the Natural Sciences and Engineering Research Council of Canada.

CM801911N